

Multiple superconducting transition in ceramic $\text{YBa}_2\text{Cu}_3\text{O}_{7-\delta}$

Dan Goldschmidt

*School of Physics and Astronomy, Raymond and Beverly Sackler Faculty of Exact Sciences,
Tel Aviv University, Tel Aviv 699778, Israel*

(Received 31 March 1988)

The temperature derivative of the resistance is utilized to investigate current density effects on the resistive superconducting transition in ceramic $\text{YBa}_2\text{Cu}_3\text{O}_{7-\delta}$. In this analysis the transition is presented as a peak with definite midpoint temperature and width. The zero-resistance and onset temperatures are also determined unambiguously. Multiple transition regimes were observed with increasing current density. A tail regime below the major transition, which is responsible for the low current densities reported by many laboratories, is shown to broaden markedly with current density. The temperature dependence of the critical current in the tail regime is close to linear above 77 K. The tail regime, that is also very sensitive to preparation and to aging through environmental attack, originates probably from Josephson-coupled, randomly oriented grain boundaries. The main transition regime, on the other hand, is quite inert to preparation and environmental contamination; it has a much higher critical current and a markedly different (i.e., non-linear) temperature dependence of the critical current near the transition. It is likely that this component of the critical current, as observed in the main transition regime, represents the intragranular critical current in ceramic superconductors.

INTRODUCTION

Already at the announcement of high- T_c superconductivity in rare-earth copper oxides made by Bednorz and Müller, current-density effects on the transition have been realized.¹ Despite a transition width of ~ 20 K in this pioneering work, a shift to lower T_c and increase in transition width with current density, typical of granular superconductors, has been observed.¹ Ever since, a great deal of effort towards improving these materials has been made resulting in a high- T_c and very sharp transition. In ceramic $\text{YBa}_2\text{Cu}_3\text{O}_{7-\delta}$, for instance, transitions at temperatures higher than 90 K and narrower than 1 K have been observed under low current-density conditions.² However, even in these improved materials one often observes a tail extending to lower temperatures in the resistive transition.³ It is with the purpose to study current-density effects on the transition and its broadening that we started this investigation.

In ceramic superconductors it is now generally accepted that the transport critical current is determined by Josephson-coupled weak links at grain boundaries. This stems from the following observations: The magnitude of the transport critical current in ceramics is quite low (100 to 1000 A/cm² at 77 K),^{3,4} and increases rapidly upon reducing the number of misoriented grain boundaries in textured ceramics ($\sim 10^4$ A/cm²),⁵ up to very high values ($> 10^6$ A/cm²) in the more perfect single crystals⁶ and thin films.⁷ Besides, there exists a strong magnetic-field dependence of the transport critical current in ceramics⁸ that weakens upon elimination of grain boundaries,⁵ suggesting again strong Josephson effects at these boundaries. It should also be noted that the critical current inferred from high-field magnetization measurements is, in ceramics, orders of magnitude higher than the transport critical current⁶ suggesting that other, possibly intragranular, defects (such as twin planes) determine the critical currents in this case. In any case, the role of the various junctions

and boundaries in determining the shape and, particularly, the sharpness of the transition needs still to be explored.

We report here on resistance (R) derivative characteristics carried out at various current densities, and on current-voltage measurements near T_c that monitor the resistive transition in superconducting ceramic $\text{YBa}_2\text{Cu}_3\text{O}_{7-\delta}$. Our measurements indicate that two kinds (at least) of defects limit the transport in the vicinity of the superconducting transition. Moreover, these defects differ markedly from one another in the magnitude and temperature dependence of their critical current and their sensitivity to preparation and environmental contamination, suggesting different morphological origins of the defects, e.g., various kinds of grain boundaries, or other, intragranular defects.

EXPERIMENT

Our samples have been prepared in the usual solid-state reaction procedure using the appropriate amounts of 99% pure powders of CuO, Ba(NO₃)₂, and Y₂O₃ heated to 180°C in air prior to weighting. The mixed powder was ground in agate mortar and pestle, fired for one day at 935°C in flowing O₂, and furnace cooled, reground, and sieved. We examined many samples, that have all been prepared from this starting material, and have shown similar response to current-density variation. We report here on two such samples that are representatives of their batches. The first ("good") sample was pressed into a disk under 6.5 kbar, sintered two days at 950°C in flowing O₂ in a quartz tube furnace, then cooled in steps: 750°C for 3 h, 550°C for 3 h, furnace cooled to 200°C (~ 4 h), and removed. The final dimensions were 9.35 mm in diameter and 0.915 mm in thickness. Estimated geometrical density was about 75% of the theoretical density. The second "poor" sample was pressed to a bar shape under a pressure of about 3 kbar. It was sintered in an Al₂O₃ boat

in the same quartz tube furnace for 21 h at 920°C in slowly flowing O₂. The cooling procedure was 4 h at 750°C, two days at 510°C, then natural furnace cooling. Final dimensions were 17×3×0.46 mm³. We have attempted to improve the preparation process of the poor samples by varying the duration and temperature of sintering (up to four days and between 900–970°C) and the cooling procedure, but the results obtained were very similar to those described below for the poor sample. The only apparent difference in preparation between the good and poor samples was a stronger O₂ flow during the sinter and cooling of the first. It is also possible that the oxygen used for the good sample was drier than for the poor ones. We have applied copper evaporated contacts to which we attached thick copper wires by pressing indium yielding an estimated contact resistance of less than 20 mΩ/contact for the good sample or by In-Ga amalgam wetting and In solder that yielded ~0.5 Ω for the poor sample. For the disk-shaped good sample, we utilized the up-down contact configuration (i.e., current contacts on one side of the disk, voltage contacts on the other), whereas for the bar-shaped poor sample, a linear configuration was used. In both samples the current contact area was between 1 and 10 mm²/contact. The Pt thin-film resistance thermometer was attached directly to the sample (that was mounted onto a thin sapphire wafer on a copper block) close to the voltage contacts using a thin Si grease layer, providing a sensitive measure of the surface temperature. In our resistance measurements, when large measuring currents were applied, the sample was first allowed to reach steady state near room temperature, then the slow cooling was initiated. In the case of current-voltage measurements that will be described elsewhere,⁹ special care was taken to avoid contact heating by using a pulsed current technique with a short duty cycle. The stability of internal temperature during the *I-V* measurement is inferred from the absence of hysteresis during increasing and decreasing of current.

The differential resistance was determined by applying both current polarities at a given current, thereby eliminating effects of slowly varying thermal voltages. The applied currents were in the 1 mA to 1 A range. The geometrical current densities (in A/cm²) may be obtained by multiplying these values by 12 and 55 for the good and

poor samples, respectively. These values of current densities are only a lower limit since in the case of the good sample, where an up-down contact configuration was used, the geometrical thickness overestimates the actual current-path thickness. Another problem in estimating current densities is sample inhomogeneity. In our samples this may be reflected in the somewhat large geometrical resistivity (~0.6 mΩ cm above the transition).

RESULTS

The conventional $R(T)$ plots for the good sample are shown in Fig. 1. The transition, which is sharp at the lowest current density, develops a low-temperature tail upon an increase in current density. The transition region is best described in terms of the derivative curve. Figure 2 shows the computed derivative $\Delta[R/R(300\text{ K})]/\Delta T$ between adjacent resistance data points for the 100 mA applied current. Thus, the superconducting transition can be described as a peak corresponding to the transition midpoint (hereafter referred to as T_c^{mid} , the critical temperature), with well-defined zero-resistance (T_c^0) and onset (T_c^{onset}) temperatures. The transition width is also easily determined in this way, e.g., 0.35 K at half maximum or 0.7 K at full width. The width of the transition is presumably related to a distribution of T_c among grains.

More insight is gained by plotting the derivative curves for various current densities on the same scale (Fig. 3). Immediately, three regimes become apparent. The first is the peak corresponding to the main portion of the transition and representing the major drop in resistance. The second corresponds to the low-temperature tail of the transition that was mentioned above; broadening of this tail is very pronounced in this presentation. The third regime is the high-temperature side of the transition, that corresponds to the region below ~120 K where $R(T)$ deviates from linearity,¹⁰ in which all derivative curves coincide to the same nonzero value.

The broadening of the derivative curves indicates that some fraction of the weak links at a given regime have undergone the superconducting to normal transition due to current density that exceeds the critical current density for these junctions. Thus variation of the measuring current may be used as a tool to probe the critical current

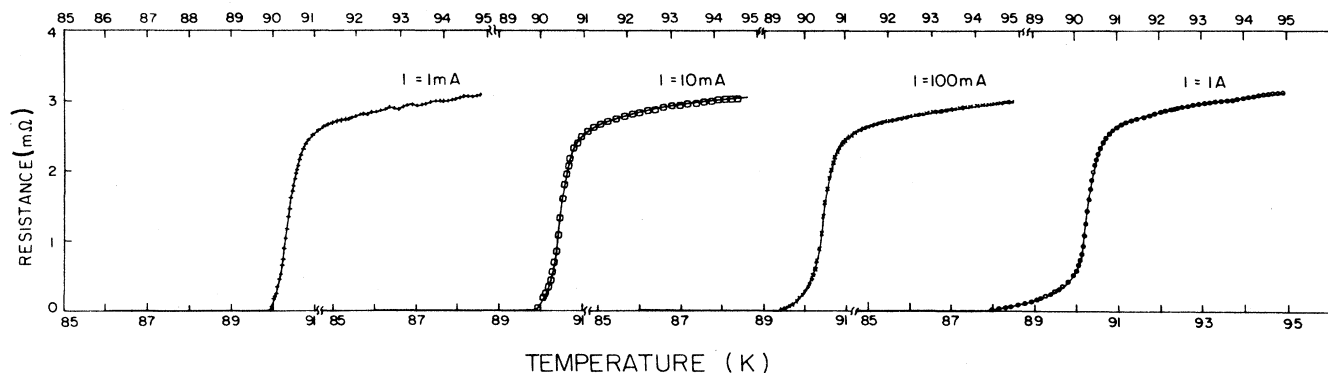


FIG. 1. Current density dependence of the resistive transition of the good sample. Notice the evolution of a low-temperature tail at high current densities.

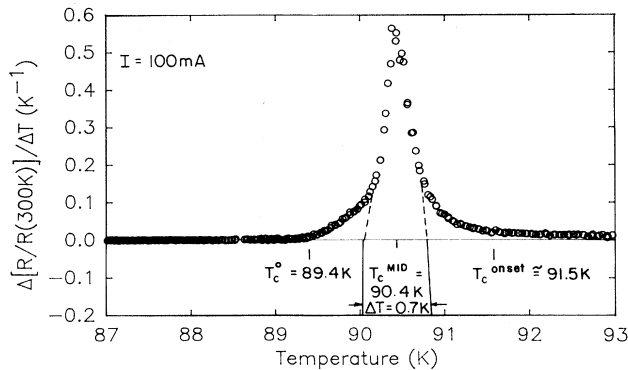


FIG. 2. Normalized resistance derivative near the transition for both sample cooling and heating. Well-defined transition temperature (T_c^{mid}) and width, zero resistance (T_c^0), and onset temperatures are obtained.

versus temperature curve, i.e., the shape of this curve may be inferred from the derivative curves, as is outlined below.

The point that we would like to emphasize is that *all three regimes have different dependences of the critical current on temperature*. First, one notes that for the tail (second) regime, a strong sensitivity to current density exists, that is, broadening occurs already for minute currents. This means that the dependence of critical current on temperature in the tail regime is smooth, i.e., no abrupt changes occur near T_c . To be more specific, we plot in Fig. 4 the dependence of T_c^0 on measuring current. The onset of finite resistance occurs just when the measuring current exceeds the critical current typical for the end of the tail regime. Thus, this curve represents the temperature dependence of the critical current density in the tail regime typical of the grain-boundary network. Within the accuracy of available data this dependence is linear. A similar dependence (i.e., with almost the same slope and intercept) is obtained by direct determination of the critical current in the tail regime from current-voltage measurements on this sample above liquid-nitrogen temperatures (see Ref. 9). The later results, that should coincide with the T_c^0 data, since both represent the onset of nonzero resistance, are also shown in Fig. 4. In other

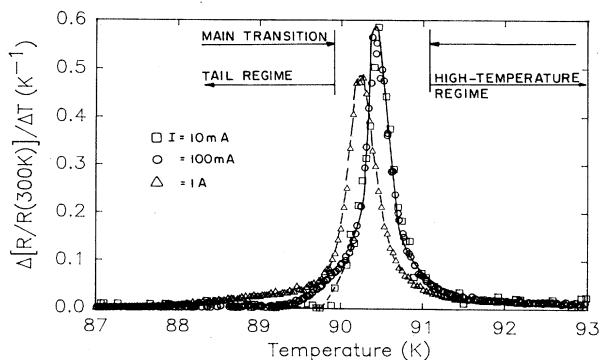


FIG. 3. Resistance derivative at various current densities. Three transition regimes, differing by response to current density, are observed. Lower limit for estimated current densities (in A/cm^2) are obtained by multiplying the currents by 12.

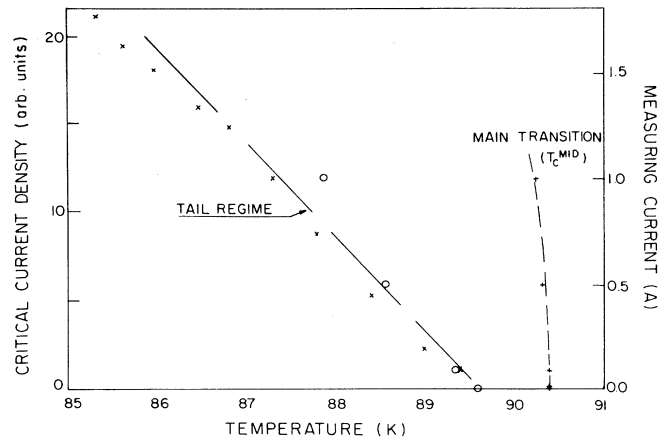


FIG. 4. Critical current densities obtained in the following ways: \times from I - V curves (Ref. 9); \circ from the current dependence of T_c^0 ; $+$ from the current dependence of T_c^{mid} .

words, and since the critical current is close to linear with temperature, increasing the measuring currents acts as probing the critical current curve at increasingly lower temperatures, providing the broadening observed in the tail regime.

In the main transition regime, on the other hand, the situation is quite different. Here, the lower current densities do not at all affect the position or width of the main peak (see Fig. 3). Only when a certain current is exceeded (in the vicinity of 1 A for the good sample) a shift in the peak position and peak broadening are observed. This implies that *close to the transition* (i.e., within less than 0.5 K below T_c^{mid} , see Fig. 4), the temperature dependence of the critical current becomes very sharp and that *the critical current drops abruptly to low values since it has to vanish at the critical temperature*. That is, increasing the measuring current in the main peak regime within a certain range of currents probes the critical current at a more or less fixed temperature, namely, the critical temperature T_c^{mid} . This unusual result is quite clear in our raw data (Fig. 3), since the peak that represents the critical temperature in the lower current curves does not shift with current. The details of the temperature dependence of this component of the critical current that represents the main transition regime, however, have to await further studies.

The third regime, at temperatures higher than the main transition, has been occasionally referred to as onset of very high-temperature superconductivity. In this case, and since the derivative curves coincide for all current densities, that is, no broadening is observed, the measuring currents seem to be much lower than the corresponding critical currents, apparently implying large critical current densities in the third regime. However, it has been suggested that the third regime, which shows a nearly logarithmic rounding near the transition, reflects superconducting fluctuation caused by pair breaking due to inelastic collisions.¹⁰ The inelastic scattering time should be independent of current density in the low electric field limit. Thus, it is more likely that the coincidence of the resistance derivatives reflects this insensitivity to current rather

er than a specific value of a critical current.

Turning now to the poor sample (Fig. 5), we notice that the results are practically unchanged for the main peak and for the high-temperature regime. For the main transition, the peak position is almost the same as in the good sample and it shifts markedly only when currents exceeding 100 mA are applied. The peak width is somewhat larger than for the good sample. However, in the low-temperature tail a pronounced broadening in the $R(T)$ curve is now observed (not shown) that is represented by a new peak in the derivative curve (Fig. 5). Besides, the tail in the derivative curve has broadened profoundly. Moreover, the sharpness and position of the secondary peak vary from sample to sample. Apparently, a new superconducting phase has precipitated, or an additional transition in the original phase has set in. For instance, regions with lower oxygen stoichiometry contain probably a lower carrier density which should yield a lower critical temperature. However, in the slow cooling applied, it is hard to realize how oxygen inhomogeneity is incorporated, particularly since the cooling procedures of the good and poor samples were quite similar. The inhomogeneity could also be attributed to humidity effects as mentioned earlier, or to other impurities. One notes though that, unlike the main peak, the secondary peak is sensitive to minute current densities similar to the tail regime in the good sample. This, together with the shape variation from sample to sample, suggests that both the tail regime and secondary peak originate from similar defects, e.g., grain boundaries and exterior regions of the grains, respectively.

DISCUSSION

The origin of the distribution of junctions in the tail regime as well as of differences between samples is of much practical importance. Several investigations on the microstructure at grain boundaries and its role in affecting the weak-link critical current have appeared in the literature.^{8,11,12} Nakahara *et al.*¹¹ have reported the existence in the same sample of various types of grain boundaries that defer by the relative orientations of the adjacent grains and by the shape of these grains. They have also observed carbon segregation at some of these grain boundaries. Depending on the nature of these boundaries (e.g., boundary thickness and conductivity) they have shown that a strong effect on the critical current may result, i.e., lowering by orders of magnitude as compared to the intrinsic depairing current. Ekin *et al.*,⁸ on the other hand, observed no impurities at grain boundaries; they attribute the low critical currents to the low current-transfer probability (as imposed by crystalline conduction anisotropy) at randomly oriented grain boundaries. Clarke¹² has recently observed the existence of two kinds of interconnected grain-boundary networks, classified primarily as large-angle and low-angle boundaries. It is likely that these different grain boundaries have different transport properties and carry different critical currents. Indeed, recent measurements on the good sample indicate some aging effect that resulted in complete elimination of the Josephson supercurrent from the current-voltage characteristics.⁹ This postpreparation aging effect may be related to

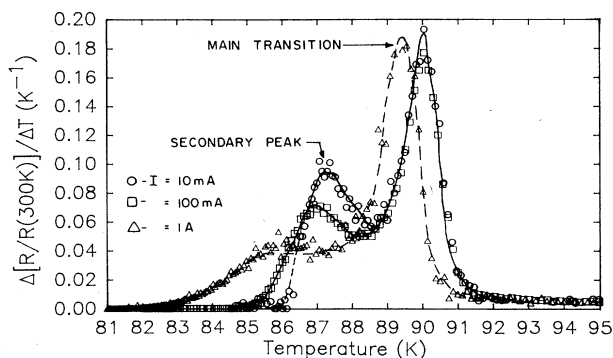


FIG. 5. Resistance derivative of the poor sample, indicating the development of a secondary peak in the tail regime.

water or other environmental impurity contamination as it occurred below room temperature. It probably indicates that the grain-boundary networks got disconnected.

More interesting is the origin of the main transition since an unusual temperature dependence of the critical current is observed in this regime and the magnitude of the critical current is markedly larger than in the tail regime. Besides, the main peak is less affected by the details of preparation or by aging. It is possible that grain boundaries that have better transport properties, e.g., the low-angle grain boundaries mentioned above are responsible for the behavior in the main transition regime. In this case, there could be within the same sample two different kinds of interconnected networks of grain boundaries that give rise to the different behavior observed in the main transition and tail regimes. However, it is more likely that the main transition regime is related to intragranular rather than to grain-boundary defects, since the drop in resistance signals the onset of superconductivity inside the grains.

In summary, we have shown by investigating current effects and by utilizing a novel derivative technique that the resistive superconducting transition in ceramic $\text{YBa}_2\text{Cu}_3\text{O}_{7-\delta}$ is a multiple transition containing a tail regime, a main transition regime, and a high-temperature regime. In some samples a secondary transition shows up in the tail regime, for which the shape and position are sample dependent. Besides, in the tail regime, pronounced broadening occurs upon increase in current density. Critical current densities usually reported in the literature correspond to this tail regime that originates from weak links at regions susceptible to impurities such as high-angle grain boundaries. On the other hand, the main transition regime, where an unusual temperature dependence of another component of the critical current density as well as larger critical currents, together with low sensitivity to impurity incorporation have been observed, reflects probably the intragranular critical current.

Note added. In a recent overnight anneal of the poor sample in flowing O_2 at 500°C , the secondary peak has been completely eliminated; the remaining main peak is, however, broader than in the good sample. This anneal suggests again that the secondary peak and tail regime are related to either lack of oxygen or impurity (water) contamination.

ACKNOWLEDGMENT

This work was supported by the United States-Israel Binational Science Foundation.

- ¹J. G. Bednorz and K. A. Müller, *Z. Phys. B* **64**, 189 (1986).
- ²D. W. Murphy, S. Sunshine, R. B. van Dover, R. J. Cava, B. Batlogg, S. M. Zahurak, and L. F. Schneemeyer, *Phys. Rev. Lett.* **58**, 1888 (1987).
- ³R. J. Cava, B. Batlogg, R. B. van Dover, D. W. Murphy, S. Sunshine, T. Siegrist, J. P. Remeika, E. A. Rietman, S. Zahurak, and G. P. Espinosa, *Phys. Rev. Lett.* **58**, 1676 (1987).
- ⁴R. K. Bordia, H. S. Horowitz, M. A. Subramanian, J. B. Michel, E. M. McCarron, III, C. C. Torardi, J. D. Bolt, U. Chowdhry, E. Lopdrup, and S. J. Poon, in *High Temperature Superconductors*, edited by M. B. Brodsky, R. C. Dynes, K. Kitazawa, and H. L. Tuller, Materials Research Society Symposium Series, Vol. 99 (Materials Research Society, Pittsburgh, 1988), p. 245.
- ⁵S. Jin, in Ref. 4, p. 773.
- ⁶T. R. Dinger, T. K. Worthington, W. J. Gallagher, and R. L. Sandstorm, *Phys. Rev. Lett.* **58**, 2687 (1987).
- ⁷P. Chaudhari, R. H. Koch, R. B. Laibowitz, T. R. McGuire, and R. J. Gambino, *Phys. Rev. Lett.* **58**, 2684 (1987).
- ⁸J. W. Ekin, A. I. Braginski, A. J. Panson, M. A. Janocko, D. W. Cappone II, N. J. Zaluzec, B. Flandermyer, O. F. deLima, M. Hong, J. Kwo, and S. H. Liou, *J. Appl. Phys.* **62**, 4821 (1987).
- ⁹D. Goldschmidt (unpublished).
- ¹⁰A. T. Fiory, A. F. Hebard, L. F. Schneemeyer, and J. V. Waszczak, in Ref. 4, p. 861.
- ¹¹S. Nakahara, G. J. Fisanick, M. F. Yan, R. B. van Dover, T. Boone, and R. Moore, *J. Cryst. Growth* **85**, 639 (1987).
- ¹²D. Clarke (private communication).